The Journal of Chemical Physics

Adsorption of common solvent molecules on graphene and MoS_2 from first-principles

Cite as: J. Chem. Phys. **149**, 094702 (2018); https://doi.org/10.1063/1.5042524
Submitted: 01 June 2018 . Accepted: 20 August 2018 . Published Online: 06 September 2018

Urvesh Patil, and Nuala M. Caffrey

Adsorption of common solvent molecules on graphene and MoS_2 from first-principles

Urvesh Patil and Nuala M. Caffrey
School of Physics and CRANN, Trinity College, Dublin 2, Ireland

(Received 1 June 2018; accepted 20 August 2018; published online 6 September 2018)

Solvents are an essential element in the production and processing of two-dimensional (2D) materials. For example, the liquid-phase exfoliation of layered materials requires a solvent to prevent the resulting monolayers from re-aggregating, while solutions of functional atoms and molecules are routinely used to modify the properties of the layers. It is generally assumed that these solvents do not interact strongly with the layer and so their effects can be neglected. Yet experimental evidence has suggested that explicit atomic-scale interactions between the solvent and layered material may play a crucial role in exfoliation and cause unintended electronic changes in the layer. Little is known about the precise nature of the interaction between the solvent molecules and the 2D layer. Here, we use density functional theory calculations to determine the adsorption configuration and binding energy of a variety of common solvent molecules, both polar and non-polar, on two of the most popular 2D materials, namely, graphene and MoS_2. We show that these molecules are physisorbed on the surface with negligible charge transferred between them. We find that the adsorption strength of the different molecules is independent of the polar nature of the solvent. However, we show that the molecules induce a significant charge rearrangement at the interface after adsorption as a result of polar bonds in the molecule. *Published by AIP Publishing.* https://doi.org/10.1063/1.5042524

I. INTRODUCTION

Two-dimensional (2D) layered materials have attracted considerable attention since the discovery of graphene due to their potential for advanced technological applications.[1–4] Yet before they can be incorporated into devices, fabrication on a cost-effective, industrial scale must be achievable. There are two general approaches to the production of isolated 2D nanolayers, namely, "top-down" and "bottom-up." Bottom-up methods comprise those which synthesize the layered material from atomic or molecular precursors and include chemical vapor deposition (CVD). While offering a high degree of atomic control, bottom-up methods generally have a prohibitively high cost.[5,6] Top-down methods involve the extraction of individual layers from a parent layered crystal. An example of this is the isolation of a graphene monolayer from graphite by micro-mechanical cleavage. While cleavage techniques have been optimized to yield high quality 2D layers, they have a relatively low yield.[7] By contrast, the liquid-phase exfoliation (LPE) of layered materials is a scalable top-down method, capable of producing industrial quantities of monolayers at a low cost.[8,9] Large shear forces, introduced in the presence of a solvent through either sonication, high-shear mixing, or wet-ball milling, are used to overcome the van der Waals (vdW) interactions binding the layers together.[10] The solvent then stabilizes the resulting nanosheets, preventing their aggregation or precipitation. Sheets with lateral sizes as large as 5 μm have been produced using this method.[11–14]

The effectiveness of LPE is critically dependent on the choice of solvent.[9,14] The simplified rule-of-thumb for solvation—that polar solvents dissolve polar solutes and non-polar solvents dissolve non-polar solutes—is no longer applicable. It was shown that matching the cohesive energies of the solute and solvent via the Hildebrand or Hansen solubility parameters can be a useful guiding principle in the search for an optimal solvent.[15] Yet this principle cannot be applied universally; in some cases, the yield can be very low despite an excellent match between the solute and solvent. For example, cyclopentanone and dimethyl phthalate have very similar Hansen and Hildebrand parameters, yet the former is one of the best solvents for the exfoliation of graphite while the latter is one of the worst.[16] The failure of these empirical solubility models suggests that considering only macroscopic solution thermodynamics is not sufficient to find good solvents.[17]

Instead, explicit structural and electronic interactions between the solvent molecules and the solute may play an important role. It has been suggested that solvent molecules can act as a "wedge," prising the layers apart at the edges, thereby improving the efficiency of subsequent exfoliation attempts.[18,19] Mutual interactions may also result in the confinement of the solvent molecules at the surface or in interlayer spaces, resulting in changes in the entropic contribution to exfoliation.[20–25]

As well as in LPE, solvents are used in a variety of different material processing and purification tasks.[26–28] In many cases, completely removing the solvent afterwards can be difficult. For example, *N*-Methyl-2-pyrrolidone (NMP) is a typical solvent used in LPE and in other solvent processing tasks, but due to its high boiling point (202 °C), it can remain as a persistent residue.[29] It is generally assumed that such

solvent molecules interact only weakly with the layered materials and so their effects can be neglected. However, this is not always the case, and given the atomic thickness and large surface area of 2D layers, there may be unintended effects on the structural and electronic properties of the layer. For example, Choi *et al.* found that common solvents can transfer sufficient charge to transition metal dichalcogenide layers to cause measurable changes in their electrical and optical properties.[30]

Very little is known about the nature of the interaction between solvent molecules and 2D layered materials on the atomic level. In this work, we use density functional theory (DFT) to systematically determine the ground state adsorption configuration of a variety of solvent molecules on two of the most widely studied 2D materials, namely, graphene and hexagonal MoS_2. We choose six representative solvents from the polar protic (2-propanol), polar aprotic [benzaldehyde, cyclopentanone, and *N*-Methyl-2-pyrrolidone (NMP)], and non-polar (toluene and chloroform) solvent families. These are shown in Fig. 1(a). Our aim is to determine whether observed differences in the ability of particular solvents to exfoliate layered materials can be attributed to differences in how individual molecules interact with the surface of that material. We determine their adsorption configuration and binding energy and show that these molecules are physisorbed on the surface with little charge transfer between the two. Despite this, a significant charge rearrangement occurs at the interface due to an induced dipole interaction.

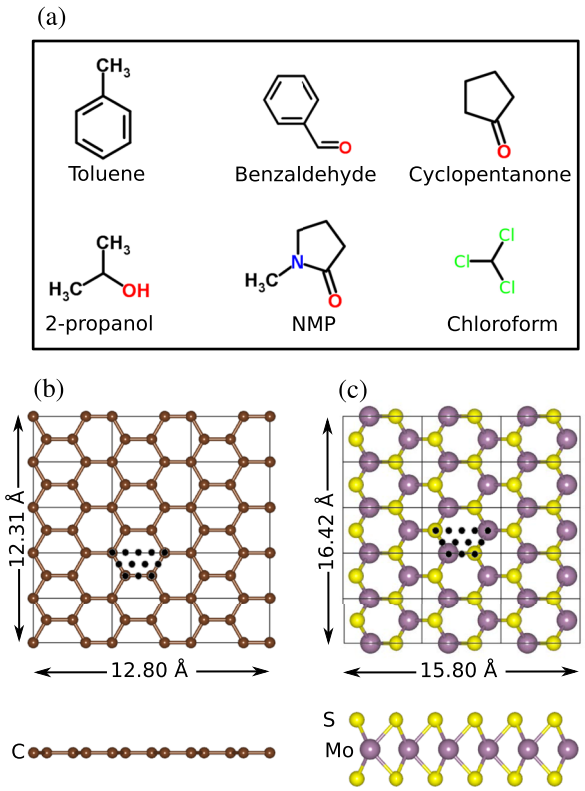

FIG. 1. (a) Geometry of the six solvent molecules considered in this study. Top and side view of the (b) graphene and (c) MoS_2 supercell used in this work. The 12 irreducible adsorption points are shown as black dots on the lattice.

II. COMPUTATIONAL METHODS

A. Density functional theory

Density functional theory (DFT) calculations are performed using the projected augmented wave (PAW) method as implemented using the VASP code.[31–34] The Perdew-Burke-Ernzerhof (PBE-PAW) potentials[35,36] provided with the package are used. The optimized optB86b-vdW functional[37–41] is used to approximate the exchange-correlation functional and to self-consistently account for van der Waals (vdW) interactions. Here, the exchange-correlation energy (E_{xc}) is given by $E_{xc} = E_x^{GGA} + E_c^{LDA} + E_c^{NL}$, where E_x^{GGA} is the exchange energy calculated using an optimized version of the B86b exchange functional,[42] E_c^{LDA} is the correlation energy calculated using the local density approximation (LDA), and E_c^{NL} is the non-local contribution to the correlation energy. This latter term encompasses the long-range interactions. The optB86b-vdW functional was previously shown to provide accurate binding energies for both gas phase clusters and bulk solids and for molecular adsorption on transition metal surfaces.[43]

In order to model the adsorption of isolated molecules, a 3×5 orthorhombic unit cell of both graphene and MoS_2 is used, as shown in Figs. 1(b) and 1(c). As a result, there is a minimum distance of at least 10 Å between periodic images of the molecules. Furthermore, a vacuum layer of at least 15 Å is included in the direction normal to the surface to ensure that no spurious interactions between repeating layers and the dipole correction are applied.

The graphene (MoS_2) Brillouin zone is sampled with a $5 \times 5 \times 1$ ($3 \times 3 \times 1$) Monkhorst-Pack mesh[44] to carry out structural relaxations to a force tolerance of 0.02 eV/Å. All atoms in the unit cell are allowed to move, including those of the substrate. The electronic properties are then calculated using a k-point sampling of $11 \times 11 \times 1$. In all cases, a plane wave cutoff of 500 eV is used to converge the basis set.

The determination of charge transfer depends sensitively on how the charge density is assigned to each atom. Here, we use both the Density Derived Electrostatic and Chemical (DDEC) net atomic charges[45] scheme as implemented in the chargemol program and the Bader partitioning scheme.[46,47]

B. Mapping the configuration space

For multi-atom adsorbents, such as the molecules considered here, there is a large phase space of possible adsorption configurations. In order to find the lowest energy binding site, we follow a process similar to the work of Åkesson *et al.*,[48] extended to include molecular rotations. Note that while the symmetry of the substrate is taken into account when creating the initial adsorption configurations, nothing is assumed about the molecular symmetry.

The following workflow is used to determine the ground state binding configuration: The individual components, i.e., the molecule and the 2D layered material, are first relaxed to determine their isolated structures. A uniform grid is then defined at a typical binding height (3.5 Å) above the surface

of each material, as shown in Figs. 1(b) and 1(c). The grid spacing is defined as $d/2$ where d is the C–C or Mo–S bond length, projected in-plane. The center of mass (COM) of each molecule is placed at each grid point.

Due to the low adsorption concentration considered here, each molecule will minimize its total energy by maximising its total area of overlap with the surface, i.e., planar molecules adsorb flat against the substrate.[49,50] With this restriction, molecular rotations, in steps of 5°, around an axis normal to the basal plane of the substrate are considered. Out-of-plane rotations are also included. Planar molecules such as benzaldehyde have only one indistinguishable out-of-plane rotation. NMP, cyclopentanone, and toluene are non-planar with two possible rotational configurations obtained by a 180° rotation out-of-plane. Chloroform has four possible rotational configurations: two in which the H–C bond is perpendicular to the plane of graphene and another two in which the H–C bond is at 60° to the plane. Finally, 2-propanol also has four possible rotational configurations: two orientations in which the C–O bond is perpendicular to the surface and another two in which it is parallel. A structure matching algorithm, as implemented in pymatgen,[51] then reduces the total number of configurations.

The total energy of each of these configurations, without relaxation, is calculated. The entire procedure is then repeated for a sub-set of these configurations at a lower height in steps of 0.25 Å until the lowest energy adsorption height is found. At this stage, a structural optimization of all structures at local minima with total energies within 0.05 eV of the global minimum is performed. The configuration with the lowest total energy after this structural optimization is the ground state configuration.

III. RESULTS AND DISCUSSION

A. Ground state configurations

The solvent molecules are found to adsorb at an average binding height of 3.35 Å from the surface of both graphene and MoS_2. The binding heights are shown in Fig. 2. The smallest binding height is found for benzaldehyde on graphene (3.00 Å), while the largest binding height of 3.56 Å is found for 2-propanol on graphene. These heights are consistent with physisorption.[48,50,52]

The potential energy surface (PES) for these molecules is four-dimensional, involving the in-plane translational coordinates as well as both in-plane and out-of-plane rotations. An example is shown in the Appendix for a fixed rotational angle.

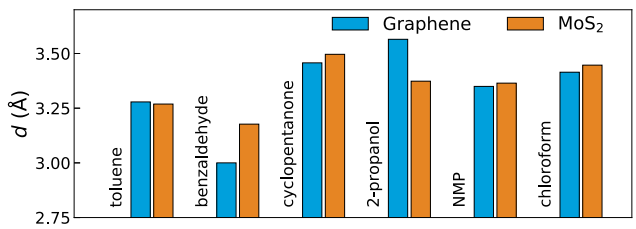

FIG. 2. The binding height of the center of mass of the molecule from the basal plane of the substrate.

In the following, we present only the final, geometrically optimized, minimum energy configurations for each of the solvent molecules. These are shown in Fig. 3.

The adsorption positions of each of the six solvent molecules adsorbed on graphene are shown in the top panel of Fig. 3. Molecules which contain a six-member ring are found to adsorb such that every alternate atom of the carbon ring is on top of a carbon atom in the graphene sheet, similar to the AB-stacking of two adjacent carbon layers in a graphite crystal.[53] This is particularly evident for toluene and benzaldehyde where small deviations from the perfect AB-type stacking are dictated by the functional group attached to the ring. The methyl group of toluene is adsorbed at a "top" position, i.e., on top of a graphene carbon atom, with the edge of the methyl group tripod facing the graphene lattice, in agreement with the work of Borck *et al.*[52] By contrast, the aldehyde (CHO) functional group of benzaldehyde is adsorbed at a hollow position. This is due to the different hybridizations of the carbon atoms in the two functional groups—the carbon atom in the methyl group is sp^3 hybridized, whereas it is sp^2 hybridized in the CHO group. As the aldehyde oxygen atom has a partial negative charge, it prefers to adsorb close to a graphene bridge site.

The carbon atoms in cyclopentanone are sp^3 hybridized with the exception of that bonded to oxygen, which is sp^2 hybridized. The three carbon atoms bonded to hydrogen atoms which point toward the graphene layer are located above hollow sites. The carbon atom bonded to a hydrogen atom which points away from the graphene layer is adsorbed above a carbon top site. The remaining electropositive carbon atom is adsorbed on a graphene top site, while the electronegative oxygen atom is located close to a graphene bridge site. Similarly, the oxygen atom in 2-propanol adsorbs close to a bridge site and all sp^3 hybridized carbon atoms avoid the top sites. It maximizes its surface contact area by adsorbing such that the C–O bond is approximately parallel to the graphene layer.

For the case of NMP, the electronegative oxygen and nitrogen atoms dictate the orientation of adsorption by adsorbing close to bridge sites. Fixing the adsorption position of these two atoms determines the orientation of the rest of the molecule. Finally, for the case of chloroform, each of the chlorine atoms adsorbs close to a hollow site, with the hydrogen pointing away from the layer in a so-called "H-up" configuration. Note that this is a different adsorption configuration to that found by Åkesson *et al.* due to the more restrictive configuration space considered in that work.[48] In all cases, the deformation in the graphene substrate is less than 0.1 Å.

The geometrically optimized configurations of the molecules adsorbed on MoS_2 are shown in the bottom panel of Fig. 3. In all cases, molecules with hydrogen atoms which point toward the MoS_2 surface prefer to adsorb such that they are located in the hollow formed by the sulfur atoms, i.e., directly on top of the metal atoms. For benzaldehyde and toluene, the carbon ring prefers to have alternate carbon atoms above the metal atoms with the center of the ring directly above a sulfur atom. Similarly, for cyclopentanone, the center of the carbon ring prefers to adsorb directly above a sulfur atom with the carbon atoms located either directly on top of the molybdenum

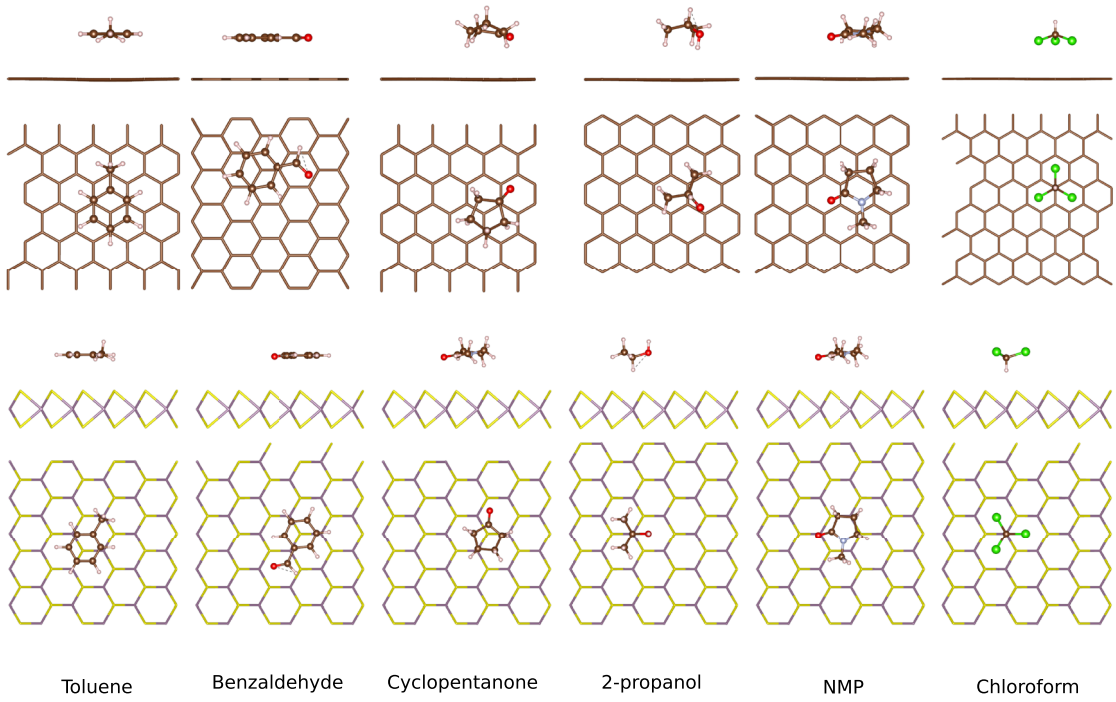

FIG. 3. Top (bottom) panel: Side and top view of the lowest energy binding site of the solvent molecule on graphene (MoS_2).

atoms or in the hollow of the substrate hexagon. 2-propanol occupies the valley created by the sulfur atoms, with the functionalized carbon atom located on top of the metal atom. Note that this is a 180° out-of-plane rotation with respect to the orientation of the same molecule on graphene. For the case of NMP, the electronegative oxygen atom is adsorbed on top of the metal atom with the orientation of the rest of the molecule dictated by the hydrogen atoms which point toward the surface.

Finally, the hydrogen atom of chloroform also prefers to adsorb in the valley created by the sulfur atoms, directly above the metal atom, so that the molecule is in a "H-down" configuration. This is in contrast to its binding configuration on graphene where it adsorbs with the hydrogen atom pointing away from the surface, i.e., "H-up." In all cases, the deformation of the MoS_2 substrate after solvent adsorption is negligible.

B. Binding energy

The binding energy between the layered material and the adsorbed solvent molecule is defined as

$$E_b = E_{\text{mol+layer}} - E_{\text{layer}} - E_{\text{mol}},$$

where E_{layer} is the total energy of the clean monolayer, E_{mol} is the total energy of the isolated molecule, and $E_{\text{mol+layer}}$ is the total energy of the combined system. The binding energies of each solvent molecule adsorbed on both graphene and MoS_2 are shown in Fig. 4(a). They range between −0.4 eV and −0.79 eV per molecule. The binding energy of each molecule differs by no more than 7% when adsorbed on graphene compared to MoS_2. The molecular binding energy rescaled by the total number of atoms in that molecule, excluding hydrogen, N, is then shown in Fig. 4(b). In all cases, the normalized binding energies lie in a narrow range between approximately 90 and 120 meV/atom and with a difference of no more than 5 meV/atom between individual molecules adsorbed on graphene and MoS_2. A similarly narrow range of normalized binding energy was found for aromatic and conjugated compounds adsorbed on MoS_2[50] and graphene[54] and shown experimentally for acenes adsorbed on copper surfaces.[55] This is evidence of the dominance of the van der Waals contribution to the binding energy. Further evidence is found by neglecting the non-local contribution to the correlation energy in the optB86b-vdW functional. In this case, a positive binding energy can be found for all the molecules considered on both surfaces. In a similar way, the interlayer binding energy

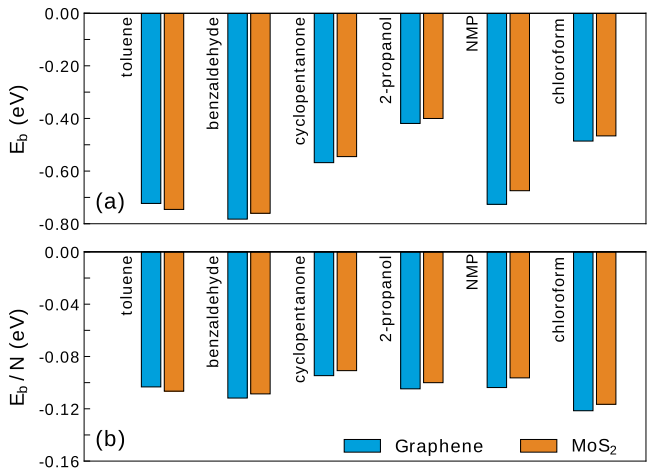

FIG. 4. (a) Binding energy of each molecule on a graphene (blue) and MoS_2 (orange) substrate. (b) Binding energies normalized by the number of non-hydrogen atoms, N, in the molecule.

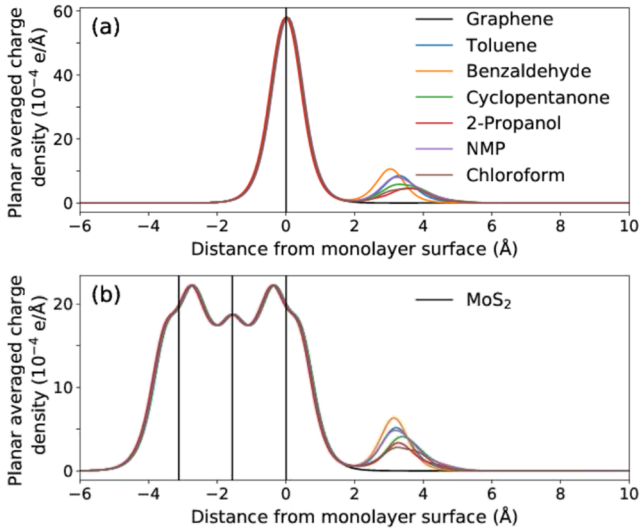

FIG. 5. Planar average of the charge density of each of the six molecules adsorbed on (a) graphene and (b) MoS_2 compared to the pristine monolayers. The vertical lines indicate the positions of atoms in the monolayers.

of graphite was previously shown to be positive using the optB86b-vdW functional when only local contributions to the correlation energy are considered.[56]

C. Charge transfer and rearrangement

The magnitude of total charge transfer between the molecules and both graphene and MoS_2 is no more than $0.11e^-$ per molecule as determined by both the Bader and the DDEC methods. In some cases, these two methods do not agree on the direction of the charge transfer. Given the difficulties in partitioning space, in order to assign charge to the molecule or substrate, this magnitude of the charge transfer may be considered essentially zero.

This is corroborated by a negligible difference in the charge density located on the monolayers before and after adsorption, as shown in Fig. 5. From this, we can conclude that the changes in the photoluminescence spectra found by Choi *et al.* after solvent adsorption on MoS_2 and attributed to charge transfer to/from the layer must be due to interactions between the solvent molecules and defects in the layers or with edge sites.[30] Such defects and edge sites have previously been shown to be considerably more reactive than the pristine surface.[57–59]

Notwithstanding the negligible charge transfer involved, significant charge reorganization occurs on both the molecule and the 2D layer as result of their interaction. To visualize this, we show in Fig. 6 a slice through the charge density difference that occurs after molecular adsorption on graphene and MoS_2 at a height of 0.5 Å above the surface of the monolayer. This height highlights the changes that occur in the outermost valance orbitals of the 2D layers. The charge density difference is defined as

$$\Delta\rho = \rho_{\text{mol+layer}} - \rho_{\text{mol}} - \rho_{\text{layer}},$$

where $\rho_{\text{mol+layer}}$, ρ_{mol}, and ρ_{layer} are the charge densities of the molecule adsorbed system, the isolated molecule, and the isolated layer, respectively. A charge rearrangement reminiscent of image charges[60] on a metal is found to occur after molecular adsorption on graphene. As a result of their high polarizabilities,[61] the substrate's charge density is modified by the polar bonds of the adsorbing molecule. This can be seen as the response of the layer to the net dipole of the molecule. The molecule then interacts with its image charge.

For the case of toluene, the small net molecular dipole points toward the methyl group. As a result, a small charge accumulation (red) is evident beneath the methyl group, and a charge depletion (blue) occurs beneath the carbon ring. This dependence of the charge rearrangement on the molecular dipole is particularly evident for molecules with an electronegative oxygen atom, such as benzaldehyde, cyclopentanone, and NMP. In these cases, charge depletion occurs beneath the oxygen atom, whereas there is charge accumulation beneath the carbon ring. This is true for those molecules adsorbed on both graphene and MoS_2. Similarly, in 2-propanol, the net dipole points away from the oxygen atom. However, the

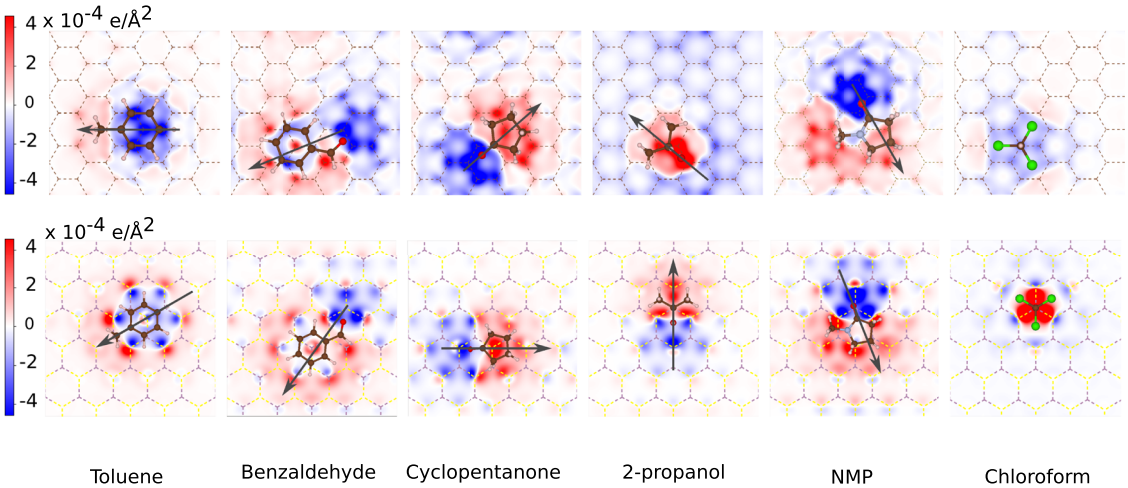

FIG. 6. Top (bottom) panel: A slice through the charge density difference 0.5 Å above the graphene (MoS_2) plane. Blue represents electron density depletion and red represents an electron density accumulation. The arrows represent the in-plane direction (but not magnitude) of the molecular dipole. The dipole of chloroform is perpendicular to the plane of the monolayer, pointing toward (away from) the layer for the case of graphene (MoS_2).

response of the 2D layer to 2-propanol depends on the out-of-plane rotation of the molecule. For the case of graphene, the molecule is adsorbed with the hydrogen atom, which is bound to the oxygen atom, pointing toward the surface. This hydrogen atom has a partial positive charge and so results in charge accumulation in the layer directly beneath it. When adsorbed on MoS_2, that hydrogen atom points away from the surface. The charge depletion in the sulfur atoms of the substrate is then obtained as a result of the partial negative charge on the oxygen atom. Finally, for the case of chloroform adsorption, the net dipole is perpendicular to the layers so that the changes in charge density around the molecule are symmetric. As the chlorine atoms have partial negative charges, charge depletion is evident directly beneath them when adsorbed on graphene, whereas there is a charge accumulation beneath the hydrogen atom which adsorbs on top of the metal atom of MoS_2.

IV. CONCLUSION

In conclusion, we have determined the adsorption configuration of six common solvent molecules on the basal plane of both graphene and MoS_2 using first-principles calculations which take van der Waals interactions into account. The calculated binding energies, adsorption heights, and charge transfer all show that the solvent molecules are physisorbed on graphene and MoS_2, with only minor variations in the binding height and binding energy between the different molecules and on the two different monolayers.

For those molecules which contain a carbon ring, we find the lowest energy adsorption configuration on graphene to be one in which a Bernal-like stacking arrangement of the carbon atoms is achieved. Non-planar molecules which have hydrogen atoms pointing toward the surface adsorb such that those atoms are located in the hollow site of the substrate lattice. We find that the orientation of both 2-propanol and chloroform is rotated by 180° when comparing adsorption on graphene and MoS_2.

Finally, despite negligible charge transfer between the solvent and monolayers, there is a significant charge rearrangement within the substrate layers in response to the partial charges on the atoms in the molecules, similar to the creation of an image charge in metals.

Liquid-phase exfoliation is strongly dependent on the type and nature of the solvent as well as the material being exfoliated. Here, we have shown that this cannot be attributed to differences in how individual molecules of that solvent interact with the surface of the 2D layer. Instead, the collective behavior of these molecules at high concentrations may play an important role.

ACKNOWLEDGMENTS

This work was supported by a Science Foundation Ireland Starting Investigator Research Grant (No. 15/SIRG/3314). Computational resources were provided by the supercomputer facilities at the Trinity Center for High Performance Computing (TCHPC) and at the Irish Center for High-End Computing (Project Nos. tcphy091b and tcphy084c). The authors would like to thank Dr. Thomas Archer for providing the "gollum" script, a modified version of which was used to perform the high-throughput calculations.

APPENDIX: POTENTIAL ENERGY SURFACE FOR CHLOROFORM

In the following, we show the PES for chloroform adsorbed on both graphene and MoS_2 at a particular rotational angle. The ground-state adsorption configuration of this molecule is rotated by 180° out-of-plane on these two surfaces. The PES for a specific rotational angle can illustrate the physical mechanism behind the differing adsorption configurations. In this case, the in-plane rotational angle is fixed at that found for the ground state configuration, as shown in Fig. 3.

The PES for chloroform adsorbed in a "H-down" configuration on graphene at a constant height of 3.5 Å is shown in Fig. 7(a). Recall that the black dots in these figures correspond to the adsorption position of the center of mass (COM) of the molecule. When the H atom is adsorbed directly above a carbon atom, the short distance between the two atoms results in a large $p_z - s$ orbital repulsion and hence a maximum in the global energy. By contrast, when the H atom is adsorbed directly above the hollow site, the distance between the H atom and the carbon atoms is large, resulting in a small $p_z - s$ orbital repulsion and thus a local minimum in the total energy.

Similarly, for the case of the "H-up" adsorption configuration [shown in Fig. 7(b)], when the three chlorine atoms are adsorbed directly above the hollow site (so that the COM of the molecule is above a carbon atom), the p_z-lone pair repulsion is minimized, resulting in the global minimum in the total energy. When the chlorine atoms are adsorbed directly above the carbon atoms, maximum p_z-lone pair repulsion occurs, leading to a local maximum in the total energy.

The PES for chloroform adsorbed in a "H-down" configuration on MoS_2 is shown in Fig. 7(c). When the H atom is

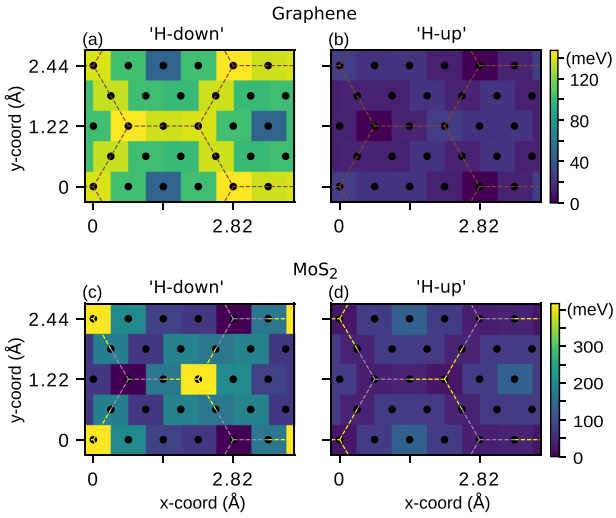

FIG. 7. Potential energy surface (PES) at a fixed in-plane rotational angle for chloroform in (a) the "H-down" configuration on graphene, (b) the "H-up" configuration on graphene, (c) the "H-down" configuration on MoS_2, and (d) the "H-up" configuration on MoS_2.

adsorbed directly above the sulfur atom (the yellow dashed lines), the small distance between the atoms results in maximum lone pair-*s* orbital repulsion and hence a global maximum in the total energy. By contrast, when the H atom is adsorbed directly above the metal atom, in the hollow formed by the sulfur atoms, four atoms are now involved in van der Waals interactions without any increase in orbital repulsion. This leads to a global minimum in the total energy.

Similarly, for the case of the "H-up" adsorption configuration [shown in Fig. 7(d)], the adsorption of the central carbon atom (and COM) directly above the metal atom results in a local maximum in energy. The minimum in energy is found when the central atom is adsorbed on top of the sulfur atom so that the chlorine atoms adsorb directly on top of the hollow site.

[1] W. Yang, L. Gan, H. Li, and T. Zhai, "Two-dimensional layered nanomaterials for gas-sensing applications," Inorg. Chem. Front. **3**, 433 (2016).
[2] M. Chhowalla, D. Jena, and H. Zhang, "Two-dimensional semiconductors for transistors," Nat. Rev. Mater. **1**, 16052 (2016).
[3] E. G. da Silveira Firmiano, A. C. Rabelo, C. J. Dalmaschio, A. N. Pinheiro, E. C. Pereira, W. H. Schreiner, and E. R. Leite, "Supercapacitor electrodes obtained by directly bonding 2D MoS_2 on reduced graphene oxide," Adv. Energy Mater. **4**, 1301380 (2014).
[4] H. Hwang, H. Kim, and J. Cho, "MoS_2 nanoplates consisting of disordered graphene-like layers for high rate lithium battery anode materials," Nano Lett. **11**, 4826 (2011).
[5] W. Choi, N. Choudhary, G. H. Han, J. Park, D. Akinwande, and Y. H. Lee, "Recent development of two-dimensional transition metal dichalcogenides and their applications," Mater. Today **20**, 116 (2017).
[6] J. Yu, J. Li, W. Zhang, and H. Chang, "Synthesis of high quality two-dimensional materials via chemical vapor deposition," Chem. Sci. **6**, 6705 (2015).
[7] K. S. Novoselov, "Nobel lecture: Graphene: Materials in the flatland," Rev. Mod. Phys. **83**, 837 (2011).
[8] V. Nicolosi, M. Chhowalla, M. G. Kanatzidis, M. S. Strano, and J. N. Coleman, "Liquid exfoliation of layered materials," Science **340**, 1226419 (2013).
[9] J. N. Coleman, "Liquid exfoliation of defect-free graphene," Acc. Chem. Res. **46**, 14 (2013).
[10] H. Tao, Y. Zhang, Y. Gao, Z. Sun, C. Yan, and J. Texter, "Scalable exfoliation and dispersion of two-dimensional materials—An update," Phys. Chem. Chem. Phys. **19**, 921 (2017).
[11] K. R. Paton, E. Varrla, C. Backes, R. J. Smith, U. Khan, A. O'Neill, C. Boland, M. Lotya, O. M. Istrate, P. King, T. Higgins, S. Barwich, P. May, P. Puczkarski, I. Ahmed, M. Moebius, H. Pettersson, E. Long, J. Coelho, S. E. O'Brien, E. K. McGuire, B. M. Sanchez, G. S. Duesberg, N. McEvoy, T. J. Pennycook, C. Downing, A. Crossley, V. Nicolosi, and J. N. Coleman, "Scalable production of large quantities of defect-free few-layer graphene by shear exfoliation in liquids," Nat. Mater. **13**, 624 (2014).
[12] U. Khan, A. O'Neill, H. Porwal, P. May, K. Nawaz, and J. N. Coleman, "Size selection of dispersed, exfoliated graphene flakes by controlled centrifugation," Carbon **50**, 470 (2012).
[13] A. O'Neill, U. Khan, and J. N. Coleman, "Preparation of high concentration dispersions of exfoliated MoS_2 with increased flake size," Chem. Mater. **24**, 2414 (2012).
[14] J. N. Coleman, M. Lotya, A. O'Neill, S. D. Bergin, P. J. King, U. Khan, K. Young, A. Gaucher, S. De, R. J. Smith, I. V. Shvets, S. K. Arora, G. Stanton, H.-Y. Kim, K. Lee, G. T. Kim, G. S. Duesberg, T. Hallam, J. J. Boland, J. J. Wang, J. F. Donegan, J. C. Grunlan, G. Moriarty, A. Shmeliov, R. J. Nicholls, J. M. Perkins, E. M. Grieveson, K. Theuwissen, D. W. McComb, P. D. Nellist, and V. Nicolosi, "Two-dimensional nanosheets produced by liquid exfoliation of layered materials," Science **331**, 568 (2011).
[15] S. D. Bergin, Z. Sun, D. Rickard, P. V. Streich, J. P. Hamilton, and J. N. Coleman, "Multicomponent solubility parameters for single-walled carbon nanotube-solvent mixtures," ACS Nano **3**, 2340 (2009).
[16] Y. Hernandez, M. Lotya, D. Rickard, S. D. Bergin, and J. N. Coleman, "Measurement of multicomponent solubility parameters for graphene facilitates solvent discovery," Langmuir **26**, 3208 (2009).
[17] J. Shen, Y. He, J. Wu, C. Gao, K. Keyshar, X. Zhang, Y. Yang, M. Ye, R. Vajtai, J. Lou, and P. M. Ajayan, "Liquid phase exfoliation of two-dimensional materials by directly probing and matching surface tension components," Nano Lett. **15**, 5449 (2015).
[18] J. Xu, D. K. Dang, V. T. Tran, X. Liu, J. S. Chung, S. H. Hur, W. M. Choi, E. J. Kim, and P. A. Kohl, "Liquid-phase exfoliation of graphene in organic solvents with addition of naphthalene," J. Colloid Interface Sci. **418**, 37 (2014).
[19] V. Sresht, A. A. Pádua, and D. Blankschtein, "Liquid-phase exfoliation of phosphorene: Design rules from molecular dynamics simulations," ACS Nano **9**, 8255 (2015).
[20] V. Arunachalam and S. Vasudevan, "Graphene–solvent interactions in nonaqueous dispersions: 2D ROESY NMR measurements and molecular dynamics simulations," J. Phys. Chem. C **122**, 1881 (2018).
[21] C. Maciel, E. E. Fileti, and R. Rivelino, "Assessing the solvation mechanism of $C_{60}(OH)_{24}$ in aqueous solution," Chem. Phys. Lett. **507**, 244 (2011).
[22] A. Govind Rajan, V. Sresht, A. A. Pádua, M. S. Strano, and D. Blankschtein, "Dominance of dispersion interactions and entropy over electrostatics in determining the wettability and friction of two-dimensional MoS_2 surfaces," ACS Nano **10**, 9145 (2016).
[23] C. A. Howard, H. Thompson, J. C. Wasse, and N. T. Skipper, "Formation of giant solvation shells around fulleride anions in liquid ammonia," J. Am. Chem. Soc. **126**, 13228 (2004).
[24] T. K. Mukhopadhyay and A. Datta, "Deciphering the role of solvents in the liquid phase exfoliation of hexagonal boron nitridse: A molecular dynamics simulation study," J. Phys. Chem. C **121**, 811 (2017).
[25] T. K. Mukhopadhyay and A. Datta, "Ordering and dynamics for the formation of two-dimensional molecular crystals on black phosphorene," J. Phys. Chem. C **121**, 10210 (2017).
[26] P. L. Cullen, K. M. Cox, M. K. Bin Subhan, L. Picco, O. D. Payton, D. J. Buckley, T. S. Miller, S. A. Hodge, N. T. Skipper, V. Tileli, and C. A. Howard, "Ionic solutions of two-dimensional materials," Nat. Chem. **9**, 244 (2017).
[27] F. Torrisi, T. Hasan, W. Wu, Z. Sun, A. Lombardo, T. S. Kulmala, G.-W. Hsieh, S. Jung, F. Bonaccorso, P. J. Paul, D. Chu, and A. C. Ferrari, "Inkjet-printed graphene electronics," ACS Nano **6**, 2992 (2012).
[28] F. Withers, H. Yang, L. Britnell, A. P. Rooney, E. Lewis, A. Felten, C. R. Woods, V. Sanchez Romaguera, T. Georgiou, A. Eckmann, Y. J. Kim, S. G. Yeates, S. J. Haigh, A. K. Geim, K. S. Novoselov, and C. Casiraghi, "Heterostructures produced from nanosheet-based inks," Nano Lett. **14**, 3987 (2014).
[29] E. P. Nguyen, B. J. Carey, T. Daeneke, J. Z. Ou, K. Latham, S. Zhuiykov, and K. Kalantar-zadeh, "Investigation of two-solvent grinding-assisted liquid phase exfoliation of layered MoS_2," Chem. Mater. **27**, 53 (2014).
[30] J. Choi, H. Y. Zhang, H. D. Du, and J. H. Choi, "Understanding solvent effects on the properties of two-dimensional transition metal dichalcogenides," ACS Appl. Mater. Interfaces **8**, 8864 (2016).
[31] G. Kresse and J. Hafner, "*Ab initio* molecular dynamics for liquid metals," Phys. Rev. B **47**, 558 (1993).
[32] G. Kresse and J. Hafner, "*Ab initio* molecular-dynamics simulation of the liquid-metal–amorphous-semiconductor transition in germanium," Phys. Rev. B **49**, 14251 (1994).
[33] G. Kresse and J. Furthmüller, "Efficiency of *ab-initio* total energy calculations for metals and semiconductors using a plane-wave basis set," Comput. Mater. Sci. **6**, 15 (1996).
[34] G. Kresse and J. Furthmüller, "Efficient iterative schemes for *ab initio* total-energy calculations using a plane-wave basis set," Phys. Rev. B **54**, 11169 (1996).
[35] P. E. Blöchl, "Projector augmented-wave method," Phys. Rev. B **50**, 17953 (1994).
[36] G. Kresse and D. Joubert, "From ultrasoft pseudopotentials to the projector augmented-wave method," Phys. Rev. B **59**, 1758 (1999).
[37] J. c. v. Klimeš, D. R. Bowler, and A. Michaelides, "Van der Waals density functionals applied to solids," Phys. Rev. B **83**, 195131 (2011).
[38] T. Thonhauser, V. R. Cooper, S. Li, A. Puzder, P. Hyldgaard, and D. C. Langreth, "Van der Waals density functional: Self-consistent potential and the nature of the van der Waals bond," Phys. Rev. B **76**, 125112 (2007).
[39] J. Klimeš, D. R. Bowler, and A. Michaelides, "Chemical accuracy for the van der Waals density functional," J. Phys.: Condens. Matter **22**, 022201 (2010).
[40] G. Román-Pérez and J. M. Soler, "Efficient implementation of a van der Waals density functional: Application to double-wall carbon nanotubes," Phys. Rev. Lett. **103**, 096102 (2009).

[41]M. Dion, H. Rydberg, E. Schröder, D. C. Langreth, and B. I. Lundqvist, "van der Waals density functional for general geometries," Phys. Rev. Lett. **92**, 246401 (2004).
[42]A. Becke, "On the large-gradient behavior of the density functional exchange energy," J. Chem. Phys. **85**, 7184 (1986).
[43]J. Carrasco, W. Liu, A. Michaelides, and A. Tkatchenko, "Insight into the description of van der Waals forces for benzene adsorption on transition metal (111) surfaces," J. Chem. Phys. **140**, 084704 (2014).
[44]H. J. Monkhorst and J. D. Pack, "Special points for brillouin-zone integrations," Phys. Rev. B **13**, 5188 (1976).
[45]T. A. Manz and D. S. Sholl, "Improved atoms-in-molecule charge partitioning functional for simultaneously reproducing the electrostatic potential and chemical states in periodic and nonperiodic materials," J. Chem. Theory Comput. **8**, 2844 (2012).
[46]M. Yu and D. R. Trinkle, "Accurate and efficient algorithm for Bader charge integration," J. Chem. Phys. **134**, 064111 (2011).
[47]W. Tang, E. Sanville, and G. Henkelman, "A grid-based Bader analysis algorithm without lattice bias," J. Phys.: Condens. Matter **21**, 084204 (2009).
[48]J. Åkesson, O. Sundborg, O. Wahlström, and E. Schröder, "A van der Waals density functional study of chloroform and other trihalomethanes on graphene," J. Chem. Phys. **137**, 174702 (2012).
[49]S. Barja, M. Garnica, J. J. Hinarejos, A. L. de Parga, N. Martin, and R. Miranda, "Self-organization of electron acceptor molecules on graphene," Chem. Commun. **46**, 8198 (2010).
[50]P. G. Moses, J. J. Mortensen, B. I. Lundqvist, and J. K. Nørskov, "Density functional study of the adsorption and van der Waals binding of aromatic and conjugated compounds on the basal plane of MoS_2," J. Chem. Phys. **130**, 104709 (2009).
[51]S. P. Ong, W. D. Richards, A. Jain, G. Hautier, M. Kocher, S. Cholia, D. Gunter, V. L. Chevrier, K. A. Persson, and G. Ceder, "Python materials genomics (pymatgen): A robust, open-source python library for materials analysis," Comput. Mater. Sci. **68**, 314 (2013).
[52]Ø. Borck and E. Schröder, "Methylbenzenes on graphene," Surf. Sci. **664**, 162 (2017).
[53]K. Yoshizawa, T. Kato, and T. Yamabe, "Interlayer interactions in two-dimensional systems: Second-order effects causing ABAB stacking of layers in graphite," J. Chem. Phys. **105**, 2099 (1996).
[54]S. D. Chakarova-Käck, A. Vojvodic, J. Kleis, P. Hyldgaard, and E. Schröder, "Binding of polycyclic aromatic hydrocarbons and graphene dimers in density functional theory," New J. Phys. **12**, 013017 (2010).
[55]S. Lukas, S. Vollmer, G. Witte, and C. Wöll, "Adsorption of acenes on flat and vicinal Cu(111) surfaces: Step induced formation of lateral order," J. Chem. Phys. **114**, 10123 (2001).
[56]G. Graziano, J. Klimeš, F. Fernandez-Alonso, and A. Michaelides, "Improved description of soft layered materials with van der Waals density functional theory," J. Phys.: Condens. Matter **24**, 424216 (2012).
[57]Z. Lin, B. R. Carvalho, E. Kahn, R. Lv, R. Rao, H. Terrones, M. A. Pimenta, and M. Terrones, "Defect engineering of two-dimensional transition metal dichalcogenides," 2D Mater. **3**, 022002 (2016).
[58]S. M. Davis and J. C. Carver, Appl. Surf. Sci. **20**, 193 (1984).
[59]G. Ye, Y. Gong, J. Lin, B. Li, Y. He, S. T. Pantelides, W. Zhou, R. Vajtai, and P. M. Ajayan, "Defects engineered monolayer MoS_2 for improved hydrogen evolution reaction," Nano Lett. **16**, 1097 (2016).
[60]S. Roychoudhury, C. Motta, and S. Sanvito, "Charge transfer energies of benzene physisorbed on a graphene sheet from constrained density functional theory," Phys. Rev. B **93**, 045130 (2016).
[61]E. J. Santos, "Electric field effects on graphene materials," in *Exotic Properties of Carbon Nanomatter* (Springer, 2015), p. 383.